

See discussions, stats, and author profiles for this publication at: <https://www.researchgate.net/publication/245292864>

# Exterior Bathymetric Effects in Elliptic Harbor Wave Models

Article in *Journal of Waterway, Port, Coastal and Ocean Engineering* · March 2000

DOI: 10.1061/(ASCE)0733-950X(2000)126:2(71)

## CITATIONS

43

## READS

120

6 authors, including:



**Vijay Panchang**

Texas A&M University - Galveston

49 PUBLICATIONS 1,161 CITATIONS

[SEE PROFILE](#)



**Kadija Schlenker**

University of Chester

2 PUBLICATIONS 43 CITATIONS

[SEE PROFILE](#)



**Zeki Demirebilek**

Engineer Research and Development Center - U.S. Army

175 PUBLICATIONS 2,023 CITATIONS

[SEE PROFILE](#)



**Michele Okihiro**

University of California, San Diego

11 PUBLICATIONS 491 CITATIONS

[SEE PROFILE](#)

Some of the authors of this publication are also working on these related projects:



Estimating runoff using 1D and 2D Boussinesq model [View project](#)



Eagle Harbor [View project](#)

# EXTERIOR BATHYMETRIC EFFECTS IN ELLIPTIC HARBOR WAVE MODELS

By Vijay Panchang,<sup>1</sup> W. Chen,<sup>2</sup> B. Xu,<sup>3</sup> K. Schlenker,<sup>4</sup> Z. Demirbilek,<sup>5</sup> and M. Okihiro<sup>6</sup>

**ABSTRACT:** Traditional elliptic harbor wave models are based on the assumptions that the region outside the computational grid is of constant depth and that the exterior coastlines are collinear and fully reflecting. These assumptions, which are associated with the open boundary, are generally not met in practice. This paper demonstrates that the effects of exterior depth variations on model results can be substantial, leading to unreliable simulations even with sophisticated modern wave models. A technique is developed to overcome these limitations. It is based on a one-dimensional representation to better simulate the effects of the exterior bathymetry. The results of the one-dimensional model are then interfaced along the open boundary of a two-dimensional finite-element harbor wave model. The new model is tested against analytical solutions for the case of wave propagation on a sloping beach, which is a difficult problem for harbor models in use today. Excellent results are obtained, suggesting that improved representation of the cross-shore slopes while treating the open boundaries may enhance the usefulness of these models.

## INTRODUCTION

The solution of the two-dimensional elliptic mild-slope wave equation is a well-accepted method for modeling surface gravity waves in harbors (Berkhoff 1976; Mei 1983; Tsay and Liu 1983; Kostense et al. 1986; Xu and Panchang 1993; Thompson et al. 1996). This equation may be written as

$$\nabla \cdot (CC_g \nabla \phi) + \frac{C_g}{C} \sigma^2 \phi = 0 \quad (1)$$

where  $\phi(x, y)$  = complex surface elevation function, from which the wave height can be estimated;  $\sigma$  = wave frequency under consideration;  $C(x, y)$  = phase velocity =  $\sigma/k$ ;  $C_g(x, y)$  = group velocity =  $\partial\sigma/\partial k$ ; and  $k(x, y)$  = wave number ( $=2\pi/L$ ), related to the local depth  $d(x, y)$  through the dispersion relation

$$\sigma^2 = gk \tanh(kd) \quad (2)$$

Eq. (1), which is applicable to a wide range of wave periods, may also be extended to include the effects of friction, breaking, and nonlinear dispersion (Chen 1986; De Giralomo et al. 1988; Panchang et al. 1991). It is usually solved by numerical techniques after separating the overall domain into two regions (Fig. 1)—the interior harbor area  $\Omega$ , which is usually represented by a finite-element or finite-difference grid; and the exterior sea  $\Omega'$ , which is often called the “superelement.” In the exterior, the wavefield  $\phi_{\text{ext}}$  consists of the specified incident wavefield  $\phi_i$ , the reflected wavefield  $\phi_r$ , and the scattered wavefield  $\phi_s$ . In the numerical solution, descriptions of these wavefields are required to interface the interior and exterior solutions along the open boundary (shown by the semicircular boundary  $\Gamma$  in Fig. 1). In traditional harbor models (Mei 1983; Tsay and Liu 1983; Thompson et al. 1996), the exterior wave conditions are described as follows:

$$\phi_i = A_i \exp[ikr \cos(\theta - \theta_i)], \text{ which is the specified input} \quad (3)$$

$$\phi_r = A_r \exp[ikr \cos(\theta + \theta_r)] \quad (4)$$

$$\phi_s = \sum_{n=0}^{\infty} H_n(kr)(A_n \cos n\theta + B_n \sin n\theta) \quad (5)$$

where  $(r, \theta)$  denotes the location of a point in polar coordinates;  $k$  = wave number;  $H_n$  = Hankel function of the first kind and order  $n$ ;  $A_n$  and  $B_n$  = unknown coefficients; and  $i = -1^{1/2}$ .

For the specified incident wave field given by (3), (4) and (5) result from the solution of the relevant eigenvalue problem [see Xu et al. (1996) for mathematical details]. In the traditional method, this eigenvalue problem, in which  $\phi_s$  and  $\phi_r$  are coupled, may be solved only under the following limitations:

1. The exterior region must have a constant depth.
2. The exterior coastlines  $A_1D_1$  and  $A_2D_2$  must be collinear.
3. The exterior coastlines  $A_1D_1$  and  $A_2D_2$  must be fully reflecting.

These assumptions are invalid for most field problems. Consequently, model results often show a high degree of contamination stemming from an unrealistic description of the exterior geometry.

To alleviate this difficulty, Xu et al. (1996) have developed a technique based on the following descriptions of the exterior waves:

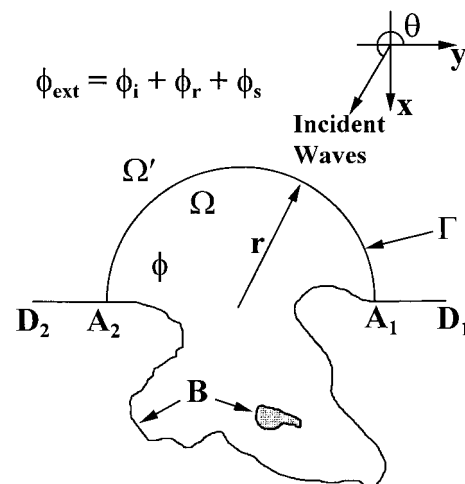


FIG. 1. Harbor Wave Model Domain; Definition Sketch

<sup>1</sup>Prof. and Program Ofcr., Nat. Sea Grant Ofc., Silver Spring, MD 20910.

<sup>2</sup>Grad. Student, Civ. Engrg. Dept., Univ. of Maine, Orono, ME 04469-5706.

<sup>3</sup>Former Grad. Student, Civ. Engrg. Dept., Univ. of Maine, Orono, ME.

<sup>4</sup>Grad. Student, Civ. Engrg. Dept., Univ. of Maine, Orono, ME.

<sup>5</sup>Res. Hydraulic Engr., U.S. Army Wtrwy. Experiment Station, Coast. and Hydr. Lab., Vicksburg, MS 39180.

<sup>6</sup>Res. Sci., School of Oc. and Earth Sci. and Technol., Univ. of Hawaii, Honolulu, HI 96822.

Note. Discussion open until September 1, 2000. To extend the closing date one month, a written request must be filed with the ASCE Manager of Journals. The manuscript for this paper was submitted for review and possible publication on July 11, 1997. This paper is part of the *Journal of Waterway, Port, Coastal, and Ocean Engineering*, Vol. 126, No. 2, March/April, 2000. ©ASCE, ISSN 0733-950X/00/0002-0071-0078/\$8.00 + \$.50 per page. Paper No. 16177.

$$\phi_r = K_r A_i \exp[ikr \cos(\theta + \theta_i)] \quad (6)$$

$$\frac{\partial \phi_s}{\partial r} = -p\phi_s - q \frac{\partial^2 \phi_s}{\partial \theta^2} \quad (7a)$$

where

$$p = -\frac{i(K^2 + k_0^2)}{2k_0} + \frac{1}{2r} - \frac{i}{8k_0 r^2}, \quad q = -\frac{i}{2k_0 r^2} \quad (7b)$$

where  $r$  and  $\theta$  represent polar coordinates of a point on the open boundary;  $k_0$  = representative constant wave number;  $K^2 = k^2 - \nabla^2(C \cdot C_g)^{1/2}/(C \cdot C_g)^{1/2}$ ; and  $K_r$  = user-specified reflection coefficient. Alternative forms of  $p$  and  $q$ , each obtained with an appropriate rationale, have been investigated by Xu et al. (1996) and Givoli (1991). Eq. (7a) is a parabolic approximation that allows the scattered waves to exit only through a limited aperture around the radial direction. Unlike (5), therefore, it does not rigorously satisfy the desired radiation properties. However, using this formulation decouples  $\phi_r$  from  $\phi_s$ ; (6) may then be obtained independently, under assumptions 1 and 2, for any desired reflection coefficient  $K_r$ . In other words, the eigenvalue problem and, hence, assumption 3 are no longer needed. For small values of  $K_r$ , (6) may be acceptable even without strict adherence to assumption 2. Xu et al. (1996) have demonstrated that a model based on this treatment yields improved solutions with less overall modeling effort than a model based on (4) and (5).

In the present paper, we tackle the problem created by assumption 1. In field applications, the exterior bathymetry is irregular and the depth generally decreases in the  $x$ -direction. This causes two problems. First, the modeler must (for both of the above techniques) arbitrarily select a representative "constant" depth and test the sensitivity of the solutions to this depth. This can be extremely time consuming. Second, the effect of the sloping exterior bathymetry is ignored in (6), leading to phase discontinuities near the open boundary. These problems are often significant, especially for long periods that are of interest in harbor resonance studies.

As an example, consider the (seemingly simple) case of one-dimensional long wave propagation over a seabed of constant slope. Under the shallow-water assumption, the one-dimensional solution for normally incident waves of frequency  $\sigma$  is

$$\Phi(x, t) = A J_0(2kx) \sin(\sigma t + \beta) \quad (8)$$

where  $\Phi$  = time-dependent form of  $\phi$ ;  $A$  and  $\beta$  = constants;  $J_0$  represents the Bessel function; and  $k$  = local wave number  $[=\sigma/(gd)^{1/2}]$ . For this analytical solution,  $x$  is the positive distance measured from the shoreline; further details regarding this solution and its application are given in Appendix I (Stoker 1958; Suhayda 1974). We solved this problem using a two-dimensional finite-element model that used (3)–(5). Results

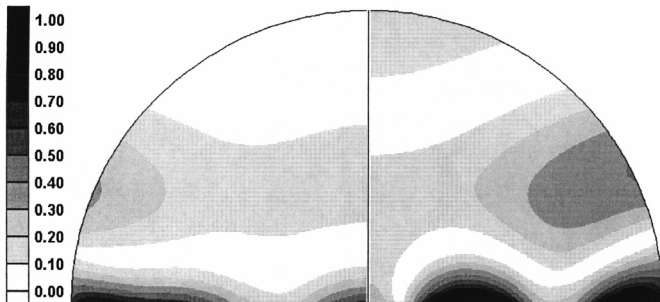


**FIG. 2. Modeled Amplification Factors; Exterior Depth Represented by (Left) Mean Depth, (Right) Maximum Depth. Waves incident from Top, Vertical Line of Symmetry Separates Half-Domain Solution Plots**

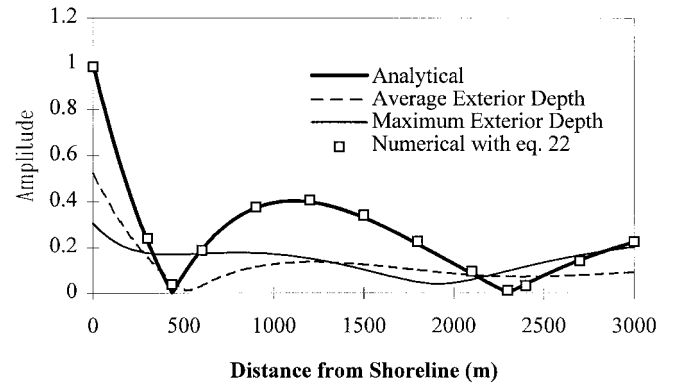


**FIG. 3. Comparison of Amplification Factors along Line of Symmetry**

from two simulations, with the exterior constant depth specified as the mean value and the largest value, are shown in Fig. 2; results along the line of symmetry are shown in Fig. 3 along with the analytical solution. It is clear that (1) the solutions are sensitive to the choice of the artificial constant depth representation; and (2) both solutions significantly differ from the desired one-dimensional analytical solution.

A technique to incorporate the exterior bathymetry in the context of a finite-element harbor wave model is developed in the next section. The "model application" section describes further development and application of this technique to appropriate test cases. Concluding remarks are given in another section.

## SOLUTION METHOD

The errors described in Figs. 2 and 3 stem from an incorrect (constant depth) representation of the exterior bathymetry. This may be overcome, of course, by incorporating the exterior depth variations in semiinfinite individual grids; the solutions may then be matched along the various interfaces (Panchang et al. 1993). As noted by Xu et al. (1996), however, such a model is extremely cumbersome to construct for routine application. We therefore consider a compromise between a detailed bathymetric representation and the unrealistic constant depth representation. We use a one-dimensional representation varying in the cross-shore direction only (Fig. 4). This is also reasonable since, in general, this is often the direction in which the nearshore depths vary the most. For the bathymetric variations shown in Fig. 4, no simple analytical expression [such as (4) or (6)] can be found for the reflected wave (Schaffer and Jonsson 1992);  $\phi_r$  must be found numerically.

For one-dimensional geometry, using Snell's law allows the incident wave potential to be written as

$$\tilde{\phi}_i = A(x) \exp \left( \int ik \cos \theta \, dx \right) \exp(iyk \sin \theta) \quad (9)$$

where  $\theta$  = incident wave angle with respect to the  $x$ -axis [see Eq. (21) in Radder (1979)]; and  $k \sin \theta$  = constant in both directions (Dean and Dalrymple 1984). The reflected wave potential is

$$\tilde{\phi}_r = B(x) \exp \left( \int -ik \cos \theta \, dx \right) \exp(iyk \sin \theta) \quad (10)$$

Therefore, the total wave potential is

$$\phi_0(x, y) = \tilde{\phi}_i + \tilde{\phi}_r = \tilde{\psi}(x) e^{iyk \sin \theta} \quad (11)$$

Substituting (11) into the mild-slope equation, we have

$$\frac{d}{dx} \left( CC_g \frac{d\tilde{\psi}}{dx} \right) + \left( \frac{C_g}{C} \sigma^2 - CC_g k^2 \sin^2 \theta \right) \tilde{\psi} = 0 \quad (12)$$

This is an ordinary differential equation requiring two boundary conditions. At the offshore (open) boundary, the total wave potential is the sum of the incident and reflected wave potentials as before; if this boundary is assumed to be located in a region of constant depth, we have

$$\phi_0 = \tilde{\psi}(x)e^{iky \sin \theta} = \phi_i + \phi_r = A_0 e^{ikx \cos \theta + iky \sin \theta} + B e^{-ikx \cos \theta + iky \sin \theta} \quad (13)$$

where  $A_0$  = incident wave amplitude. Without loss of generality, the offshore boundary may be set at  $x = 0$ ; we can then eliminate  $B$  as follows (Booij 1981; Panchang et al. 1991):

$$\frac{\partial \tilde{\psi}}{\partial x} = ik \cos \theta (2A_0 - \tilde{\psi}) \quad \text{at } x = 0 \quad (14)$$

At the coastline boundary, the following approximate boundary condition given by Isaacson and Qu (1990) and Tsay and Liu (1983) may be used:

$$\frac{\partial \tilde{\psi}}{\partial x} = \frac{i\sqrt{k^2 - k^2 \sin^2 \theta}(1 - K_r)}{1 + K_r} \tilde{\psi} \quad \text{at the coastline} \quad (15)$$

where  $K_r$  = reflection coefficient.

The elliptic (12) along with the boundary conditions (14) and (15) may be solved easily by finite differences using a tridiagonal solver. The value of  $\phi_0 = \phi_i + \phi_r$  along various points of the semicircle may then be found from (11).

The balance of the exterior wavefield consists of  $\phi_s$ , which is given by (7a). Note that (5) cannot be used, since it is derived only for constant exterior depths (Xu et al. 1996). A boundary condition along  $\Gamma$  for the internal variable  $\phi$  may be obtained as follows by using the principle of the continuity of the wave potential and its derivative:

$$\frac{\partial \phi}{\partial n} = \frac{\partial \phi_0}{\partial n} + \frac{\partial \phi_s}{\partial n} \quad (16)$$

Using (7a) to describe the scattered potential yields

$$\frac{\partial \phi}{\partial n} = \frac{\partial \phi_0}{\partial n} - p\phi_s - q \frac{\partial^2 \phi_s}{\partial \theta^2} \quad (17)$$

Since  $\phi_s = \phi - \phi_0$ , (17) may be rewritten as

$$\frac{\partial \phi}{\partial n} = \frac{\partial \phi_0}{\partial n} + p\phi_0 + q \frac{\partial^2 \phi_0}{\partial \theta^2} - p\phi - q \frac{\partial^2 \phi}{\partial \theta^2} \quad \text{along } \Gamma_1 \quad (18)$$

Eq. (18), to which  $\phi_0$  data are supplied from the one-dimensional calculation described earlier, constitutes the desired open boundary condition for the solution of (1) in the harbor domain  $\Omega$ . The other boundary conditions for coastlines, islands, etc. inside  $\Omega$  is

$$\frac{\partial \phi}{\partial n} = \alpha \phi \quad (19)$$

where  $\alpha = ik(1 - K_r)/(1 + K_r)$ ; and  $K_r$  = (specified) reflection coefficient (Tsay and Liu 1983).

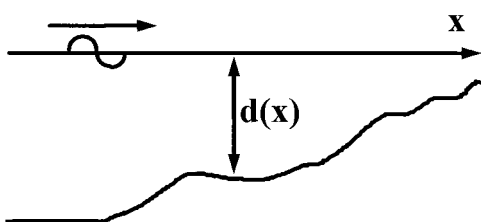


FIG. 4. 1D Representation of Exterior Bathymetry

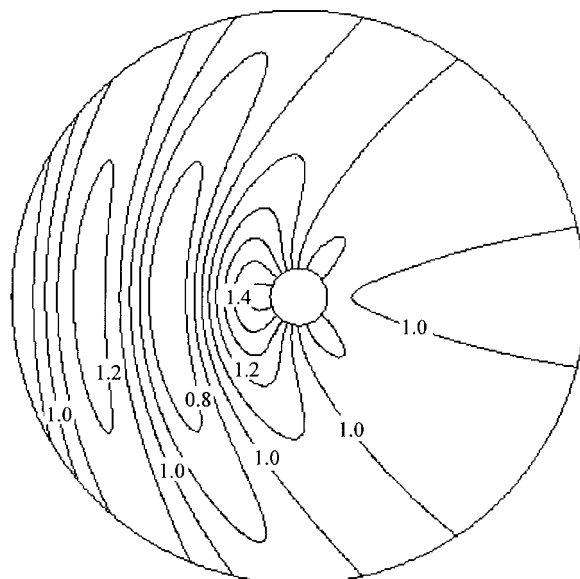


FIG. 5. Normalized Wave Heights: Waves Incident from Left

It remains to solve (1) with the boundary conditions (18) and (19) using finite elements. The complexity of (18) precludes the development of a suitable functional, however. The Galerkin technique (weak form) for the finite-element formulation (Zienkiewicz and Taylor 1989; Reddy and Gartling 1994) was therefore used along with linear triangular elements to discretize the model domain. For most field applications, wavelength dependent resolution is required; Thompson et al. (1996) suggest a minimum of six grids per wavelength. Our research suggests that at least 10 grids per wavelength are usually necessary. This requirement leads to an extremely large system of equations that is solved by iterative techniques developed specially for the mild-slope equation (Panchang et al. 1991). Tools associated with the Surface Water Modeling System (SMS) developed at Brigham Young University, Provo, Utah, facilitated the generation of wavelength-dependent grids. For examples, see Xu et al. (1996) and Panchang et al. (1999).

## MODEL APPLICATION

The long-wave sloping-beach problem described in the first section was first investigated. However, we encountered considerable difficulty in obtaining satisfactory solutions. Model solutions contained excessive amounts of spurious oscillations. These oscillations, which appeared to emanate from the near-shore areas of the open boundary, were more pronounced for the longer wave periods. This condition is probably caused by the limitations of the parabolic approximation in treating the off-axis components of waves radiating out largely in the alongshore direction, since these components experience the greatest depth changes. It is possible that a more rigorous parabolic approximation that includes depth variations to a higher level than (7a) may eliminate these numerical difficulties. However, such a parabolic approximation would entail greater complexities in combining the boundary conditions representing  $\phi_0$  and  $\phi_s$  with the internal finite-element equations. It was therefore decided to drop the second-order derivative terms in the open boundary condition and to use a lower-order approximation for  $\phi_s$ . For (7a) this gives

$$p = -ik + \frac{1}{2r} \quad \text{and} \quad q = 0 \quad (20)$$

Although this amounts to a relaxation of the parabolic approximation [(7a)], it affects only one component of the overall exterior solution (i.e.,  $\phi_s$ ) for cases where variations in the

other component (namely,  $\phi_r$ ) are dominant. This type of relaxed boundary condition has also been used by Panchang et al. (1991). The reader is also referred to Behrendt (1985) and Givoli (1991).

To investigate (only) the effects of the relaxation of the  $\phi_r$  boundary condition noted above, two well-known scattering problems with no bathymetric reflections were considered. The first problem concerns wave scattering by a circular cylinder of radius  $R_c$  in a domain of radius  $R_b$ . The incident wave period was 10 s ( $k = 0.0576$ ). An analytical solution in terms of Bessel functions is available for this situation (Berkhoff 1976; Mei 1983), which allows one to evaluate the performance of the approximate boundary conditions. Fig. 5 shows the analytical solution and the results of the model run with (7b) and (20) for  $R_c/R_b = 0.1$ . All three results are practically indistinguishable. When the cylinder is moved off center, the performance of the approximate models deteriorates somewhat. This is seen in Fig. 6, which shows asymmetry about the horizontal axis for both the parabolic [Fig. 6(a)] and relaxed [Fig. 6(b)] boundary conditions. While the results of the relaxation do appear to be inferior to the parabolic approximation, the differences are minor and reasonably good results are obtained even though the cylinder was placed at a distance of only  $2R_c$  from the open boundary. Further, it is clear, by comparing to Fig. 5, that increasing the distance of the open boundary will product satisfactory results.

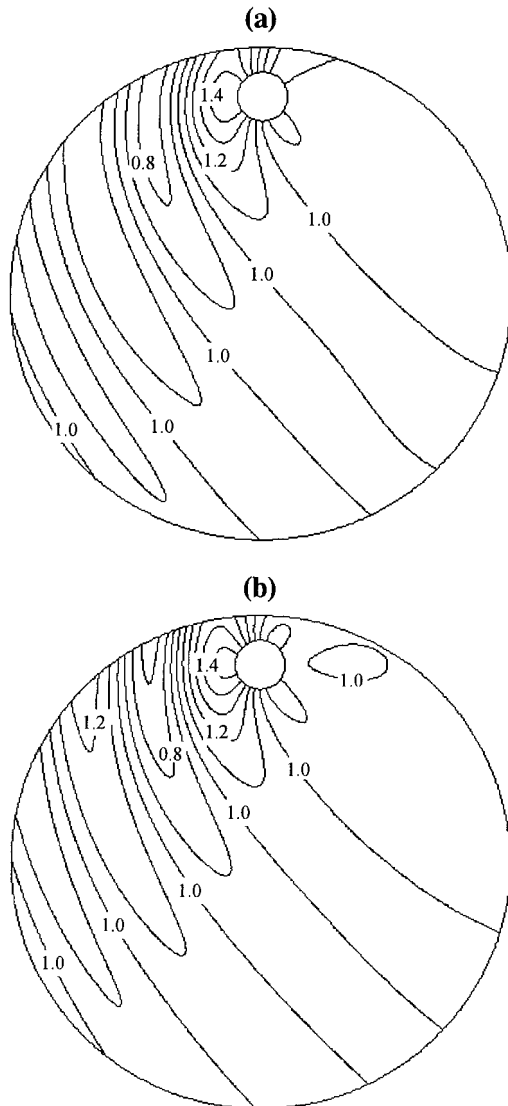


FIG. 6. Normalized Wave Heights with Boundary Condition: (a) (7b); (b) (20)

Resonance in a fully reflecting rectangular harbor of constant depth (Fig. 7) was also simulated (Mei 1983). For the first resonant peak (period of 11.1 s), which is usually difficult to simulate properly [as noted by Xu et al. (1996) and others], the correct solution obtained via (3)–(5) is shown in Fig. 8 for the central (cross-shore) line of symmetry BA. Solutions obtained with the rigorous form (7b) and its relaxation noted above are also shown, for open boundaries of various sizes. In Fig. 8, the domain sizes are denoted by  $R$  = the radius of the semicircle and  $L$  = the wavelength (150 m). In both cases,

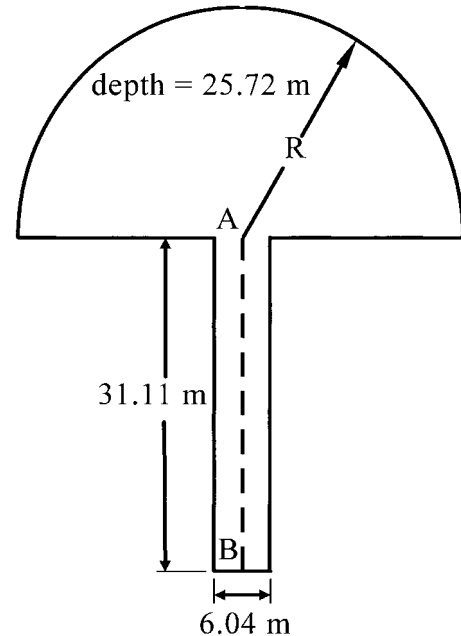


FIG. 7. Rectangular Harbor Model Domain; Waves Incident from Top

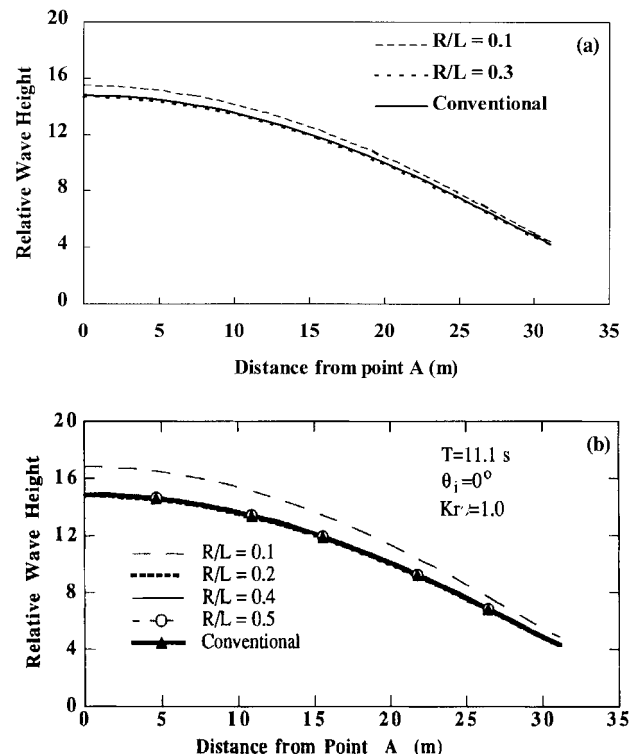


FIG. 8. Comparison of Amplification Factors Along Axis of Symmetry: (a) Traditional (Correct) Solution versus Relaxed Form of (7a); (b) Traditional (Correct) Solution versus Radial Parabolic Boundary Condition [(7a)] from Xu et al. (1996)

the solutions are seen to converge to the correct solution at roughly the same rate when the lateral extent of the domain is increased. Importantly, they are devoid of spurious oscillations that could stem from artificial reflections from the open boundary.

The method developed in the solution method section was then applied to the plane sloping beach test case mentioned in the first section. To avoid the singularity at the coastline, the domain was cut off at a minimum depth of 0.9 cm and a reflection coefficient of 1 was assigned along this boundary. At the seaward end, the depth was assumed to be constant (=54 m) beyond a distance of 3,000 m from the shoreline. [A constant depth is required in this region not only to fix the analytical solution, as noted in Appendix I, but also to satisfy (14).] A wave period of 260 s was considered. For normally incident waves of amplitude = 0.15 m (see Appendix I), modeled solutions are shown in Fig. 9 for a domain of radius  $R = L_1/2 = 3$  km. In contrast to the solutions obtained with the traditional model (Fig. 2, where also  $R = L_1/2$ ), it is clear that these solutions are completely one-dimensional and uncontaminated by open boundary effects. The results along the central cross-shore line of symmetry, shown in Fig. 3, produce a perfect match with the analytical solution.

The case of oblique incidence, which is more vulnerable to spurious boundary effects than is the case of normal incidence, was next examined. The case of short waves ( $T = 6$  s) propagating at an incident angle of  $60^\circ$  on the same sloping bathymetry described earlier was considered; however, the domain radius  $R = 200$  m and the nearshore boundary was assumed to be fully absorbing. The resulting phase diagram

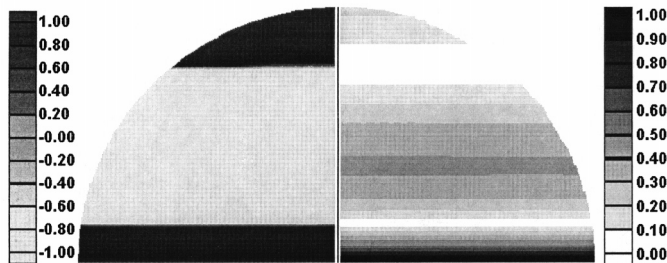


FIG. 9. Sloping Beach with Waves Incident from Top, Modeled (Left) Phase and (Right) Amplitude; Vertical Line of Symmetry Separates Half-Domain Solution Plots

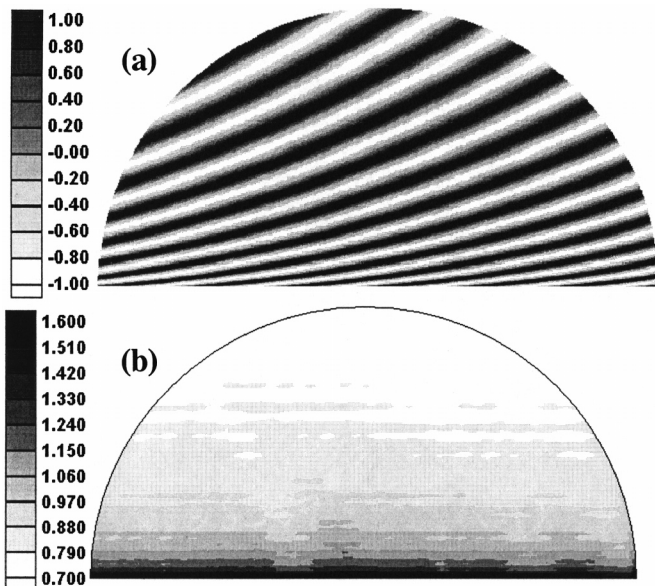


FIG. 10. Modeled: (a) Phase; (b) Amplitude for Case of Short Waves,  $\theta = 60^\circ$

for a nearshore cutoff depth of 9.0 cm, shown in Fig. 10(a), clearly indicates the expected bending of rays as described by Snell's law. The modeled amplitudes [Fig. 10(b)] are also largely one-dimensional; the solutions along the central axis of symmetry are compared with the analytical solution for shoaling and refraction (Radder 1979) in Fig. 11. Imperfections in the modeled solutions in Fig. 10 are due to inherent differences between the numerical and analytical treatment of the wave condition at the nearshore boundary. In the numerical treatment, the waves are assumed to be fully absorbed with a constant depth [(14)], whereas the analytical solution ignores this boundary and reflections from the shallow nearshore region. This was verified by changing the minimum depth at the nearshore boundary for the numerical solution; a shallower depth of 0.9 cm increased the errors [Fig. 11(b)]. In other words, the problems solved by each method are somewhat different from each other.

To further examine the modeling technique, the problem of wave reflection, refraction, and diffraction around a thin shore-connected breakwater [Fig. 12(a)] was considered. Analytical solutions for this case are described by Liu et al. (1979) and Kirby (1986) for short period waves. In our numerical simulations, the downwave boundary was placed at a depth of 0.0015 m and was assumed to be fully absorbing. The thin breakwater, which is 4.572 m long, was given a width of 0.012 m and was assumed to be fully reflecting. The radius of the open boundary was 6.096 m. In total 24,220 nodes were used in the finite-element simulation, which gave a resolution of approximately 10 points per wavelength, for the highest period considered. Simulations were performed for the three periods ( $T = 0.75$  s, 1.0 s, and 1.5 s) and two incident wave angles ( $20^\circ$  and  $30^\circ$ ) studied by Kirby (1986). Results of the modeling method described in the second section compared well with the analytical solutions for all cases. As an illustration, wave height comparisons are shown in Fig. 12(b) for the shortest and longest period along two shore-parallel transects for an incident wave direction of  $20^\circ$ . While differences in amplitude modulations between the analytical solution and the modeling method of the second section do exist, they are of the same order as those seen in higher-order parabolic approximation models (Kirby 1986); from the viewpoint of the more versatile elliptic models, however, the inclusion of the exterior depths as described above leads to a significant improvement compared with the traditional constant exterior depth models. This may be seen in Fig. 12(b) for  $T = 1.5$  s.

Finally, the model was applied to Ponce de Leon Inlet (Flor-

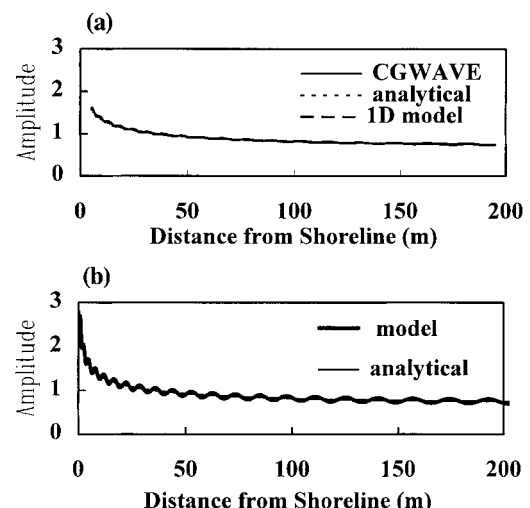
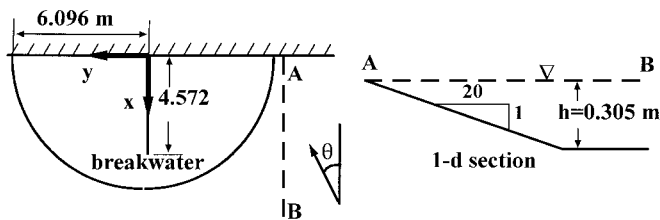


FIG. 11. Analytic and Numeric Solutions Along Central Section for Depth at Coastline of: (a) 9.0 cm (Curves Practically Identical); (b) 0.9 cm



**FIG. 12(a). Simulation for Wave Propagation Around Shore-Connected Breakwater: Problem Geometry**

ida), of which a detailed study is being conducted by the U.S. Army Corps of Engineer. The geometry consists of an exposed coastline, an inlet leading to the Halifax and Indian Rivers, a jetty with a scoured area to its side, a shoal some distance away from the tip of the jetty, and a bathymetry that is generally sloping in the off-shore direction (Smith and Harkins 1997). The model was run with the traditional constant depth representation using (7a) for the open boundary condition. The resulting phase diagram, shown in Fig. 13(a), appears fairly reasonable; however, diffraction effects due to the discontinuous bathymetry cause a break in the phases near the open

boundary. When the exterior depths are incorporated, the resulting solution is devoid of such spurious effects [Fig. 13(b)]. In addition to the phase discontinuities, the constant depth representation also influences amplitude modulations to a considerable distance inside the domain (not shown).

## SUMMARY AND CONCLUDING REMARKS

Two-dimensional elliptic models traditionally used for simulating wave conditions in harbors are adversely impacted by unrealistic assumptions about the exterior domain (Thompson et al. 1996). Xu et al. (1996) have developed a procedure to incorporate realistic exterior boundary reflectivities. That development has been extended here to allow a representative of the varying bathymetry instead of the traditional constant depth representation. The procedure consists of using a cross-shore one-dimensional bathymetric representation and first estimating  $\phi_0$  via the one-dimensional mild-slope wave equation. These values of  $\phi_0$  are then interfaced with the two-dimensional model along the open boundary. For this treatment, the parabolic boundary conditions for  $\phi_s$  developed by Xu et al. (1996) may have to be relaxed somewhat along the cross-shore

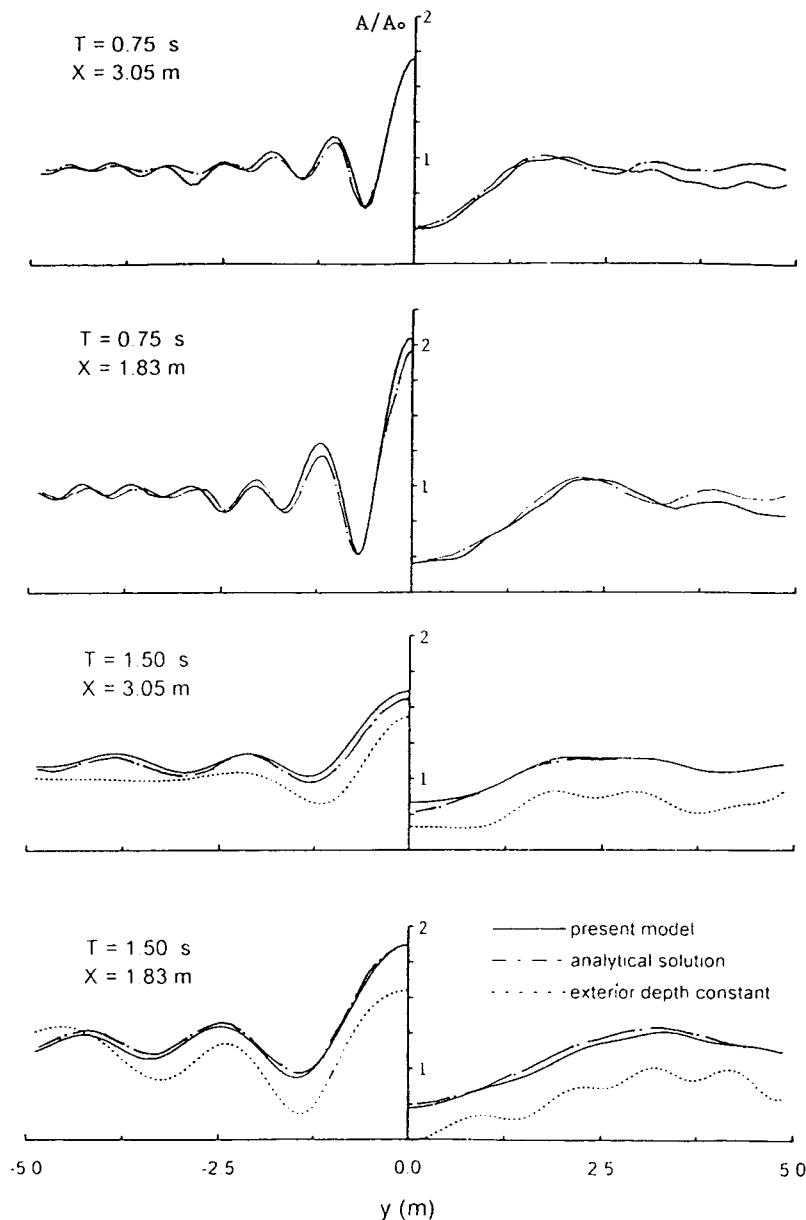


**FIG. 12(b). Simulation for Wave Propagation around Shore-Connected Breakwater: Relative Wave Height Comparisons**

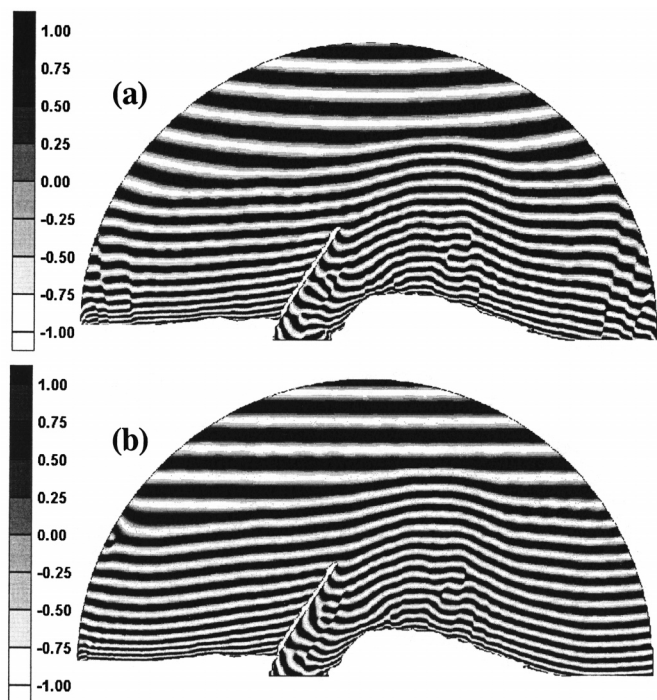


FIG. 13. Modeled Phase Diagrams for Ponce de Leon Inlet, 15 s Waves Incident from Top; Exterior Depth Representation: (a) Constant; (b) Varying in Cross-Shore Direction

boundaries in cases of steep exterior slopes. If reflections from the exterior bathymetry are not important, the more rigorous formulation of  $\phi_s$  [i.e., (7a)] may, of course, be used; the modeler may decide which approach to use on the basis of a separate one-dimensional calculation to first estimate the magnitude of the bathymetric reflections.

The modeling technique developed here was tested against analytical solutions for long waves on a plane sloping beach. Although seemingly simple, this test poses much difficulty for two-dimensional elliptic harbor wave models currently in use (Thompson et al. 1996; Xu et al. 1996). The new procedure was found to produce nearly perfect results. For the test case with a partially adsorbing coastal boundary, simulations for domains of different sizes were found to be inconsistent and acceptable. In all cases, the spurious boundary effects were extremely limited, even when the lateral extent of the domain was of the order of one wavelength (or smaller).

This study was motivated by the need to properly model long wave effects in harbors in Hawaii and California (Okiihiro et al. 1993). The periods of interest range from 30 s to 1,000 s (Okiihiro and Guza 1996); these waves experience considerable reflection by the bathymetry (Guza and Thornton 1985; Elgar et al. 1994), which in turn influences the results in the interior (harbor) domain. The results of detailed modeling studies for Kahului Harbor (Hawaii) and for Ponce de Leon Inlet will be described elsewhere.

## APPENDIX I. EQ. (8): ELABORATION

Eq. (8) may be obtained by first substituting a time-harmonic solution of the form  $\Phi = a(x)\sin \sigma_t + b(x)\cos \sigma_t$  in the one-dimensional long wave equation  $\Phi_{xx} = (C^2\Phi_x)_x$  and then specifying  $C_2 = gh(x) = gmx$ , where  $m$  is the uniform bottom slope and  $x$  is the distance from the shoreline. (Here,  $x$  is assumed to be positive offshore and  $x = 0$  at the shoreline.) This leads to Bessel's equation for  $a$  and  $b$ , and Bessel function results for each can be combined to obtain (8). In (8),  $A$  is the solution at  $x = 0$ .

As noted by Stoker (1958), however, formulations like (8)

can be explicitly used only if the waves far offshore are assumed to be simple progressive waves. Beyond  $x = x_0$ , therefore, we assume a constant depth where the solution consists of an incident wave  $\Phi_i = a \sin(kx + \sigma_t)$ , with the amplitude of a specified a priori, and a reflected wave  $\Phi_r = a \sin(kx - \sigma_t + \epsilon)$ . Matching the solution and its derivative at  $x = x_0$  gives the following relations:

$$\beta = (\pi - \epsilon)/2$$

$$\tan(kx_0 + \epsilon/2) = -J_0(2kx_0)/J_1(2kx_0)$$

$$A\{[J_0(2kx_0)]^2 + [J_1(2kx_0)]^2\}^{1/2} = 2a$$

For the problem described in the introduction and model application section,  $x_0 = 3,000$  m, and at this location  $k = 0.00105$   $\text{m}^{-1}$  for a period of 260 s. From the last relation give above, an incident amplitude of  $a = 0.15$  m is necessary to obtain  $A = 1$  m (the solution at the coast). This value of incident amplitude is chosen for numerical simulations of this test case.

## ACKNOWLEDGMENTS

Partial support for this work was received from the Maine and California Sea Grant Programs, the U.S. Army Corps of Engineers, the Office of Naval Research, and the Center for Marine Studies at the University of Maine. Comments of two anonymous reviewers were instrumental in improving this paper.

## APPENDIX II. REFERENCES

- Behrendt, L. (1985). "A finite element model for water wave diffraction including boundary absorption and bottom friction." *Ser. Paper 37*, Institute of hydrodynamics and Hydraulic Engineering, Technical University of Denmark.
- Berkhoff, J. C. W. (1976). "Mathematical models for simple harmonic linear water waves: Wave reflection and diffraction," *Publ. 163*, Delft Hydraulics Laboratory, Delft, The Netherlands.
- Booij, N. (1981). "Gravity waves on water with non-uniform depth and current." *Rep. 81-1*, Department of Civil Engineering, Delft University of Technology, Delft, The Netherlands.
- Chen, H. S. (1986). "Effects of bottom friction and boundary adsorption on water wave scattering." *Appl. Oc. Res.*, 8(2), 99–104.
- Chen, H. S., and Houston, J. R. (1987). "Calculation of water level oscillations in harbors." *Instructional Rep. CERC-87-2*, U.S. Army Corps of Engineers Waterways Experiment Station, Vicksburg, Miss.
- Dean, R. G., and Dalrymple, R. A. (1984). *Water wave mechanics for engineers and scientists*, Prentice-Hall, Englewood Cliffs, N.J.
- De Giralomo, P., Kostense, J. K., and Dingemans, M. W. (1988). "Inclusion of wave breaking in a mild-slope model." *Computer modeling in ocean engineering*, Schrefler and Zienkiewicz, eds., Balkema, Rotterdam, The Netherlands, 221–229.
- Demirebilek, Z., Xu, B., and Panchang, V. G. (1996). "Uncertainties in the validation of harbor wave models." *Proc., 25th Int. Conf. on Coast. Engrg.*
- Elgar, S. T., Herbers, H. C., and Guza, R. T. (1994). "Reflection of ocean surface gravity waves from a natural beach." *J. Phys. Oceanography*, 24(7), 1503–1511.
- Givoli, D. (1991). "Non-reflecting boundary conditions." *J. Computational Phys.*, 94, 1–29.
- Guza, R. T., and Thornton, E. B. (1985). "Observations of surf beat." *J. Geophys. Res.*, 90(c2), 3161–3172.
- Isaacson, M., and Qu, S. (1990). "Waves in a harbour with partially reflecting boundaries." *Coast. Engrg.*, 14, 193–214.
- Jones, N. L., and Richards, D. R. (1992). "Mesh generation for estuarine flow modeling." *J. Wtrwy., Port, Coast., and Oc. Engrg.*, ASCE, 118(6), 599–614.
- Kirby, J. T. (1986). "Higher-order approximations in the parabolic equation methods for water waves." *J. Geophys. Res.*, 91(c1), 933–952.
- Kostense, J. K., Meijer, K. L., Dingemans, M. W., Mynett, A. E., and van den Bosch, P. (1986). "Wave energy dissipation in arbitrarily shaped harbours of variable depth." *Proc., 20th Int. Conf. on Coast. Engrg.*, 2002–2016.
- Liu, P., L.-F., Lozano, C. J., and Pantazaras, N. (1979). "An asymptotic theory of combined wave refraction and diffraction." *Appl. Oc. Res.*, 1, 137–146.
- Mei, C. C. (1983). *The applied dynamics of ocean surface waves*, Wiley, New York.

- Okihiro, M., and Guza, R. T. (1996). "Observations of Seiche forcing and amplification in three small harbors." *J. Wtrwy., Port, Coast., and Oc. Engrg.*, ASCE, 122(5), 232–238.
- Okihiro, M., Guza, R. T., and Seymour, R. J. (1993). "Excitation of Seiche observed in a small harbor." *J. Geophys. Res.*, 122(5), 232–238.
- Panchang, V. G., Pearce, B. R., Ge, W., and Cushman-Roisin, B. (1991). "Solution to the mild-slope wave problem by iteration." *Appl. Oc. Res.*, 13(4), 187–199.
- Panchang, V. G., Xu, B., and Cushman-Roisin, B. (1993). "Bathymetric variations in the exterior domain of a harbor wave model." *Proc., Int. Conf. on Hydros. and Engrg.*, S. Wang, ed., 1555–1562.
- Panchang, V. G., Xu, B., and Demirbilek, Z. (1999). "Wave predictions models for coastal engineering applications." *Development in offshore engineering*, J. B. Herbich, ed., Gulf Publishing Co., Book Div., Houston, 163–194.
- Radder, A. C. (1979). "On the parabolic equation method for water-wave propagation." *J. Fluid Mech.*, 95, 159–176.
- Reddy, J. N., and Gartling, D. K. (1994). *The finite element method in heat transfer and fluid dynamics*. CRC, Boca Raton, Fla.
- Schaffer, H. A., and Jonsson, I. G. (1992). "Edge waves revisited." *Coast. Engrg.*, 16, 349–368.
- Smith, S. J., and Harkins, G. S. (1997). *Proc., Waves 1997*.
- Stoker, J. J. (1958). *Water waves*. Wiley, New York.
- Suhayda, J. N. (1974). "Standing waves on beaches." *J. Geophys. Res.*, 79(21), 3065–3071.
- Thompson, E. F., Chen, H. S., and Hadley, L. L. (1996). "Validation of numerical model for wind waves and swell in harbors." *J. Wtrwy. Port, Coast., and Oc., Engrg.*, ASCE, 122(5), 245–257.
- Tsay, T.-K., and Liu, P. L.-F. (1983). "A finite element model for wave refraction and diffraction." *Appl. Oc. Res.*, 5(1), 30–37.
- Xu, B., and Panchang, V. C. (1993). "Outgoing boundary conditions for finite-difference elliptic water-wave models." *Proc., Royal Soc. of London, Ser. A*, 441, 575–588.
- Xu, B., Panchang, V. G., and Demirbilek, Z. (1996). "Exterior reflections in elliptic harbor wave models." *J. Wtrwy., Port, Coast., and Oc., Engrg.*, ASCE, 122(3), 118–126.
- Zienkiewicz, O. C., and Taylor, R. L. (1989). *The finite element method*, 4th Ed., McGraw-Hill, New York.